Fermi National Accelerator Laboratory

FERMILAB–PUB–87/66–T

June, 1987

ON THE DETECTION OF ULTRAHIGH ENERGY NEUTRINOS

M. H. RENO AND C. QUIGG
Fermi National Accelerator Laboratory*
P. O. Box 500, Batavia, Illinois 60510

June 15, 1987

ABSTRACT

Cross sections for the interactions of ultrahigh energy neutrinos with nucleons are evaluated using contemporary information about nucleon structure functions. For 10^{19} eV neutrinos, the cross section is an order of magnitude larger than the values traditionally used in astrophysical calculations. Some consequences for interaction rates in the earth and for event rates in large-scale acoustic and electronic detectors from generic astrophysical neutrino sources are noted.

PACS numbers: 98.60Df, 13.15Em, 95.30Cq

I. INTRODUCTION

Recent observations[1] of neutrinos correlated with supernova SN 1987a have extended the range of observational neutrino astronomy beyond the solar system and confirmed the utility of large-volume detectors for that purpose. The neutrinos in question, most of which are presumed to be electron antineutrinos, typically have energies on the order of tens of MeV, characteristic of neutrinos produced in e^+e^- annihilations during the supernova collapse. The discovery of neutrino radiation by the large detectors gives new encouragement to the long-standing hope[2-4] of detecting ultrahigh-energy (UHE: $\gtrsim 10^{12}$ eV) cosmic neutrinos from sources beyond the atmosphere: astrophysical neutrinos associated with γ-ray point sources like Cygnus X-3[5], the isotropic ($\sim 10^{18}$ eV) neutrino flux produced[6,7] in the interactions of extragalactic cosmic rays with the microwave background, or a diffuse UHE neutrino flux associated with the decay of superconducting cosmic strings in the relatively late Universe.[8] This paper is devoted to a survey of rates for interactions of UHE neutrinos and their implications for detector characteristics.

New understanding of the characteristics of nucleon structure functions at large scales Q^2 and small momentum fractions x has made possible improved estimates[9,10] of the inclusive cross section for the reaction $\nu_\mu N \rightarrow \mu^- + \text{anything}$. In a recent paper,[10] Quigg, Reno, and Walker presented a detailed calculation of the charged current cross sections for neutrinos and antineutrinos at energies ranging from 10^9

to 10^{19} eV. The calculation is straightforward in principle, following from standard electroweak theory and the renormalization group-improved parton model. In practice, however, there are subtleties associated with the ultra-high energies considered, and at the highest energies the resulting cross sections are more than an order of magnitude larger than the cross sections previously used in many astrophysical applications. The results of Ref. 10 make precise the remark of Andreev, Berezinsky, and Smirnov[11] that the growth with increasing Q^2 of parton distributions at small Bjorken x enhances the cross section.

The enhanced charged current cross section has implications for event rates in underground detectors which were explored briefly in our earlier work[10] and in work by Gaisser and Grillo.[12] The increased cross section boosts interaction rates, but also raises the opacity of the earth to incident neutrinos and thus increases the attenuation of the neutrino beam *en route* to a detector. Both effects must be considered in analyzing the expectations for a specific experimental situation.

In this paper we extend the results of Ref. 10 in several important ways. In § II we review the calculations of the charged current cross section of Ref. 10 and compute the UHE neutral current cross section as well. Although for the moment neutral current interactions of cosmic neutrinos appear considerably more difficult to detect than the charged current interactions, this information is of potential value both for interaction rates and for the question of beam attenuation in the earth.

Section III deals briefly with the interaction lengths of UHE neutrinos in the earth. At the highest energies we consider, $\sim 10^{19}$ eV, the earth is opaque to neutrinos. We calculate event rates for the interactions of cosmic neutrinos in large underwater acoustic detectors in §IV. Then in §V we discuss discovery limits as a function of the volume of a detector for point and isotropic sources with a variety of energy spectra. Our conclusions are presented in §VI.

II. THE TOTAL NEUTRINO CROSS SECTION

It is straightforward to calculate the inclusive cross section for the reaction

$$\nu_\mu N \to \mu^- + \text{anything}, \tag{2.1}$$

where $N \equiv \dfrac{n+p}{2}$ is an isoscalar nucleon, in the renormalization group-improved parton model. The differential cross section is written in terms of the Bjorken scaling variables $x = Q^2/2M\nu$ and $y = \nu/E_\nu$ as

$$\frac{d^2\sigma}{dxdy} = \frac{2G_F^2 ME_\nu}{\pi}\left(\frac{M_W^2}{Q^2+M_W^2}\right)^2\left[xq(x,Q^2) + x(1-y)^2\overline{q}(x,Q^2)\right], \tag{2.2}$$

where $-Q^2$ is the invariant momentum transfer between the incident neutrino and outgoing muon, $\nu = (E_\nu - E_\mu)$ is the energy loss in the lab (target) frame, M and M_W are the nucleon and intermediate boson masses, and $G_F = 1.16632 \times 10^{-5}$ GeV^{-2}

is the Fermi constant. The quark distribution functions are

$$\begin{aligned} q(x,Q^2) &= \frac{u_v(x,Q^2)+d_v(x,Q^2)}{2} + \frac{u_s(x,Q^2)+d_s(x,Q^2)}{2} + s_s(x,Q^2) + b_s(x,Q^2) \\ \overline{q}(x,Q^2) &= \frac{u_s(x,Q^2)+d_s(x,Q^2)}{2} + c_s(x,Q^2) + t_s(x,Q^2), \end{aligned} \tag{2.3}$$

where the subscripts v and s label valence and sea contributions, and u, d, c, s, t, b denote the distributions for various quark flavors in a *proton.*

At low energies ($E_\nu \ll M_W^2/2M$) and in the parton-model idealization that quark distributions are independent of Q^2, the differential and total cross sections are proportional to the neutrino energy. Up to energies $E_\nu \sim 10^{11}$ eV, the familiar manifestation of the QCD-evolution of the parton distributions is to decrease the valence component, and so to decrease the total cross section. At still higher energies, the gauge boson propagator restricts $Q^2 = 2ME_\nu xy$ to values $\lesssim M_W^2$, and so limits the effective interval in x to the region $x \lesssim M_W^2/2ME_\nu$. At modest values of Q^2, the effect of this damping is to further diminish the cross section below the point-coupling, parton model approximation. Andreev, Berezinsky, and Smirnov[11] have pointed out that the growth with increasing Q^2 of parton distributions at small x enhances the cross section. Using the parton distributions available to them, Andreev, *et al.* found neutrino cross sections 2–3 times larger than the scaling prediction, for $E_\nu = 10^{17}$ eV.

Knowledge of the quark distribution functions has advanced markedly over the eight years since the publication of Ref. 11. For applications to high-energy collider physics, the QCD-evolution of the quark distributions has been studied by Eichten, Hinchliffe, Lane, and Quigg[13] (*EHLQ*) for $10^{-4} < x < 1$ over the range $5\ \mathrm{GeV}^2 < \mathrm{Q}^2 < 10^8\ \mathrm{GeV}^2$. The resulting distributions, which include the perturbatively induced heavy quark flavors, make possible an improved estimate of the neutrino cross section. This is made timely by the appearance of increasingly capable detectors for cosmic neutrinos.

For neutrino energies up to about 10^{17} eV, the *EHLQ* parton distributions contain all the information required to evaluate the neutrino cross sections. At higher energies the effect of the intermediate boson propagator is to emphasize contributions from the region $x < 10^{-4}$, outside the range of validity of the *EHLQ* distributions.[14] For such small values of x, the behavior of the parton distributions at values of Q^2 large compared to the QCD scale can be calculated, as described in detail by Gribov, Levin, and Ryskin.[15] The double logarithmic approximation (DLA) is used to sum the "most leading" contributions to parton distribution functions. For $Q^2 \sim M_W^2$, the DLA solution should be trustworthy so long as $x \gg 10^{-8}$. The combination of the DLA parametrization with the *EHLQ* quark distributions thus covers the full range of x and Q^2 relevant to the UHE νN cross section for astrophysical applications. In utilizing the DLA form we follow the suggestion of McKay and Ralston[9] who based upon it an analytic estimate of the UHE neutrino cross section. The comparison between our methods and results was given in Ref. 10.

The calculations we report employ Set 2 of the *EHLQ* structure functions for $x > 10^{-4}$. We thus include the full Q^2-evolution of the parton distribution functions for both sea and valence quarks. For smaller values of x (which contribute significantly only for neutrino energies in excess of 10^{17} eV) we use for each quark and antiquark flavor i the DLA expression of Gribov, Levin, and Ryskin[15] and McKay and Ralston[9]:

$$xq_s^i(x,Q^2) = C^i(Q^2)\left(\frac{2(\xi-\xi_0)}{\rho}\right)^{1/2}\exp\left[\sqrt{2\rho(\xi-\xi_0)}\right], \tag{2.4}$$

where

$$\begin{aligned}\rho &= \frac{8N_c}{b_0}\log\frac{1}{x}\\ \xi(Q^2) &= \log\log\frac{Q^2}{\Lambda^2}.\end{aligned} \tag{2.5}$$

Here $N_c = 3$ is the number of colors and $b_0 = (11N_c - 2n_f)/3$ for n_f flavors (for this application, 5). For the *EHLQ* distributions, the QCD scale parameter is $\Lambda = 290$ MeV and $\xi_0 = \xi(Q_0^2) = \xi(5\ \text{GeV}^2)$. The small-$x$ extrapolations of the structure functions are normalized so that for $x_0 = 10^{-4}$, we have $x_0q_s^i(x_0,Q^2)^{DLA} = x_0q_s^i(x_0,Q^2)^{EHLQ}$. This fixes the normalization $C^i(Q^2)$ for each value of Q^2. Numerical integrations were carried out using the adaptive Monte Carlo routine VEGAS.[16]

Cross sections for charged current scattering of neutrinos and antineutrinos from isoscalar nucleons are shown as dotted lines in Fig. 1. At the highest energies, where the contributions of valence quarks are unimportant, the neutrino and antineutrino cross sections are identical. At the highest energy displayed, $E_\nu = 10^{19}$ eV, these results are as much as an order of magnitude larger than parametrizations widely used in astrophysical calculations. For a complete comparison and references to earlier work, see Ref. 10.

A parallel calculation leads to the neutral current cross section. In this case the differential cross section for the reaction $\nu_\mu N \to \nu +$ anything is given by

$$\frac{d^2\sigma}{dxdy} = \frac{G_F^2 M E_\nu}{2\pi}\left(\frac{M_Z^2}{Q^2+M_Z^2}\right)^2\left[xq^0(x,Q^2) + x(1-y)^2\bar{q}^0(x,Q^2)\right], \tag{2.6}$$

where M_Z is the mass of the neutral intermediate boson. In this case the parton distribution functions are

$$\begin{aligned} q^0(x,Q^2) &= \left(\frac{u_v(x,Q^2)+d_v(x,Q^2)}{2} + \frac{u_s(x,Q^2)+d_s(x,Q^2)}{2}\right)(L_u^2+L_d^2) + \\ &\quad \left(\frac{u_s(x,Q^2)+d_s(x,Q^2)}{2}\right)(R_u^2+R_d^2) + \\ &\quad (s_s(x,Q^2)+b_s(x,Q^2))(L_d^2+R_d^2) + (c_s(x,Q^2)+t_s(x,Q^2))(L_u^2+R_u^2) \end{aligned} \tag{2.7}$$

$$\begin{aligned} \bar{q}^0(x,Q^2) &= \left(\frac{u_v(x,Q^2)+d_v(x,Q^2)}{2} + \frac{u_s(x,Q^2)+d_s(x,Q^2)}{2}\right)(R_u^2+R_d^2) + \\ &\quad \left(\frac{u_s(x,Q^2)+d_s(x,Q^2)}{2}\right)(L_u^2+L_d^2) + \\ &\quad (s_s(x,Q^2)+b_s(x,Q^2))(L_d^2+R_d^2) + (c_s(x,Q^2)+t_s(x,Q^2))(L_u^2+R_u^2), \end{aligned} \tag{2.8}$$

where the chiral couplings are

$$\begin{aligned} L_u &= 1 - \frac{4}{3}x_W \\ L_d &= -1 + \frac{2}{3}x_W \\ R_u &= -\frac{4}{3}x_W \\ R_d &= \frac{2}{3}x_W \end{aligned} \tag{2.9}$$

and $x_W = \sin^2\theta_W$ is the weak mixing parameter. For numerical calculations we have chosen $x_W = 0.226$.[17] The dashed lines in Fig. 1 show the neutral current cross sections. The summed neutral and charged current cross sections are displayed as solid lines.

III. THE EARTH IS OPAQUE TO UHE NEUTRINOS

The rise of neutral-current and charged-current cross sections with increasing energy makes the probability of neutrino-nucleon interactions in a fixed target volume increase, and so the interaction length

$$\mathcal{L}_{\text{int}} = \frac{1}{\sigma_{\nu N}(E_\nu)N_A}, \tag{3.1}$$

where $N_A = 6.022 \cdot 10^{23}$ is Avogadro's number, decreases. The interaction lengths for neutrinos in the earth are plotted in Fig. 2 as a function of the neutrino energy E_ν. For reference, we indicate as a dashed line the earth's diameter (3.4×10^9 cm.w.e.)

in centimeters of water equivalent. Above $E_\nu \simeq 10^{15}$ eV, the interaction length is smaller than the earth's diameter. The cross sections, and hence interaction lengths, for antineutrinos are equal to those for neutrinos above about 10^{14} eV.

To make our remarks about the opacity of the earth more quantitative, we show as a function of zenith angle θ in Fig. 3 the shadowing factor

$$\frac{dS}{d\Omega} = \exp(-\ell\sigma_{\nu N}(E_\nu)N_A) = \exp(-\ell/\mathcal{L}_{\text{int}}), \tag{3.2}$$

integrated over azimuth, for several values of E_ν. Here

$$\ell = \sqrt{(R_\oplus - d)^2\cos^2\theta + 2dR_\oplus - d^2} - (R_\oplus - d)\cos\theta \tag{3.3}$$

is the distance traveled through the earth, $R_\oplus$ is the radius of the earth and d is the depth of the detector. At $E_\nu = 10^{13}$ eV there is very little shadowing. Above 10^{15} eV, shadowing is substantial. At each energy, zenith angles between 90° and the angle indicated by a black dot contribute to half the total upward flux for an isotropic source.

IV. UNDERWATER ACOUSTIC DETECTORS

The larger neutrino cross section implied by the QCD evolution of the structure functions makes feasible underwater acoustic detection of the diffuse cosmic flux of UHE neutrinos.[18] The DUMAND project[19] may include a microphone array sensing a volume of 100-1000 km^3 of water at a depth of several kilometers. The energy threshold for efficient detection of charged current neutrino interactions is expected to be at neutrino energies on the order of 10^{16}–10^{17} eV. At these very high energies, the dominant conventional source of neutrinos is from very high energy protons scattering off microwave photons, producing charged pions that subsequently decay and produce neutrinos. This is the mechanism responsible for the cutoff in the primary proton spectrum at $E_p \sim 10^{20}$ eV.[20] Acoustic detection of these neutrinos would provide important information about models of galaxy formation and evolution.

Recently Hill and Schramm[7] have reconsidered the flux of cosmic ray neutrinos, taking account of pion photoproduction, pair-production reactions, and cosmological effects. An essential ingredient is the flux of cosmic protons through the microwave background, which may be inferred from current observations or from cosmological models of galactic evolution. For example, "bright phase" models[21] suggest that at earlier epochs, the brightness of galaxies was enhanced relative to their present brightness, and that the luminosity of galaxies in UHE cosmic rays follows their optical luminosity. Models of cosmic protons are parametrized in terms of $\overline{z}$, the redshift of maximum activity, and γ_i, the spectral index of the cosmic ray protons. We take as characteristic values $\overline{z} = 4$ and 6. Current observations suggest[22] that $\gamma \simeq 3$ for UHE protons, but the inferred index of the injection spectrum before passage through the microwave background can only be constrained in the range from $\gamma_i \sim 1.5 - 3$. Figure 4 shows the Hill-Schramm neutrino flux for these redshifts as well as for the case of neutrinos associated with only the observed high-energy proton spectrum, labeled by $\bar{z} = 0$. The spectra plotted are for electron neutrinos or antineutrinos; the flux of muon neutrinos would be about a factor of two higher.

We use this diffuse neutrino flux to calculate the number of events that may be observed in an underwater acoustic detector. The interaction rate in a volume V of water is

$$\Gamma = \int_{E_\nu^{\rm min}} dE_\nu \, d\Omega \, j_\nu(E_\nu) \, \sigma_{\nu N}(E_\nu) \frac{dS(E_\nu, \Omega)}{d\Omega} N_A V, \tag{4.1}$$

where 10^{16} eV$\lesssim E_\nu^{\rm min} \lesssim 10^{17}$ eV is the energy at which the detector becomes sensitive, and the shadowing factor $\dfrac{dS(E_\nu, \Omega)}{d\Omega}$ is given by (3.2). As examples of the event rates to be expected, we take $V = 100 \text{ km}^3$, although a volume as large as 1000 km^3 may be reasonable. We assume a depth $d = 4000$ m, but the results are relatively insensitive to this choice, so long as $d \ll R_\oplus$.

The calculated event rates for $\bar{z} = 0$, 4, and 6 are shown in Tables 1–3 for injection spectra with indices γ_i between 1.5 and 3. In addition to the results calculated with the shadowing factor (3.2), we show the event rates that would arise if there were no attenuation of the incident beam, *i.e.* for $dS/d\Omega = 1$. The comparison shows that the earth is nearly opaque to the neutrino beam at these energies, so that essentially all the interactions are initiated by downward-going neutrinos.

For $\overline{z} = 0$, the event rates are insensitive to $E_\nu^{\min}$ because the flux is flat out to $E\nu \simeq 2 \cdot 10^{18}$ eV, so that most of the events come from energies considerably above $E_\nu^{\min}$. For the bright phase models, the interaction rate decreases significantly if $E_\nu^{\min}$ exceeds 10^{17} eV, as the flux drops rapidly above 10^{17} eV. Tables 2 and 3 contain event rates for $E_\nu^{\min} = 10^{16}$ and 10^{17} eV, where the sensitivity to $E_\nu^{\min}$ is not extreme.

For $\overline{z} = 0$, the calculated neutrino flux is normalized to the observed spectrum of protons. High energy protons accelerated at large distances from the earth are screened by the intervening material. Therefore the *observed* proton flux represents only protons accelerated locally, within some characteristic distance R_L of the earth. However, protons accelerated out to the Hubble radius R_H will produce neutrinos in their inelastic encounters with the intervening material. The neutrinos will pass unabsorbed to the earth. Hence the $\overline{z} = 0$ neutrino spectrum should be enhanced by a factor $R_H/R_L \simeq 20$. Even with this enhancement, we expect only a few events per year for $E_\nu^{\min} > 10^{16}$ eV and the most generous case of an injection spectrum with index $\gamma_i = 1.5$.

The situation is much more promising for the bright phase models, provided the detection threshold can be set at 10^{17} eV or below. Except for the case $\gamma_i = 3.0$ at $\overline{z} = 4$, we expect at least a handful of events with the 100 km^3 volume assumed for the detector. At the other extreme of $\gamma_i = 1.5$ and $\bar{z} = 6$, a 1 km^3 detector would suffice for initial studies.

Atmospheric neutrinos are a negligible background at these very high energies. We take as the flux of atmospheric muon-neutrinos and antineutrinos[23] for $E_\nu >$ 10^{16} eV

$$j_\nu(E_\nu) \simeq 30 \cdot \left(\frac{E_\nu}{10^{16}\ \mathrm{eV}}\right)^{-4} \left(\mathrm{km}^2\ \mathrm{yr}\ \mathrm{sr}\ 10^{18}\ \mathrm{eV}\right)^{-1}. \tag{4.2}$$

The flux of electron-neutrinos at $E_\nu = 10^{16}$ eV is about a factor of forty smaller. With an energy threshold of $E_\nu^{\mathrm{min}} = 10^{16}$ eV, approximately 0.1 event per year would occur in the generic acoustic detector we have considered. Increasing the threshold by an order of magnitude decreases the event rate by almost three orders of magnitude.

V. DISCOVERY LIMITS

Thus far, the discussion of neutrino-induced event rates has relied upon a specific but conventional model of the source of UHE neutrinos, the scattering of high energy protons on the cosmic microwave background radiation. As a final application of the neutrino total cross sections, we consider event rates for an unspecified isotropic source characterized by a spectral index γ and normalization $\mathcal{N}$:

$$j_\nu(E_\nu) = \mathcal{N} \left(\frac{E_\nu}{10^{9}\ \mathrm{eV}}\right)^{-\gamma} \left(\mathrm{km}^2\ \mathrm{yr}\ \mathrm{sr}\ 10^{18}\ \mathrm{eV}\right)^{-1}. \tag{5.1}$$

As an initial step toward defining the detector parameters required for observation of a given flux j_ν, we evaluate the event rate as a function of the flux normalization $\mathcal{N}$, the spectral index γ, and the effective volume of the detector.

Let us consider an isotropic flux of muon neutrinos characterized by (5.1). The rate of charged current events is given by (4.1); as a reasonable first approximation we take the effective volume V to be independent of neutrino energy. We now ask what combination of flux normalization and volume will result in the detection of at least one upward-going muon per year, for a given spectral index. The results are shown as solid lines in Fig. 5 for various values of the minimum neutrino energy $E_\nu^{\rm min}$ required for detection. This provides a rough and generic way of taking into account different detector thresholds. For comparison, we also show as the dashed lines in Fig. 5 the value of $\mathcal{N}V$ required for one downward-going charged current event per year, for which there is no screening by the earth. At $E_\nu^{\rm min} \gtrsim 10^{15}$ eV, the effects of screening are manifest.

For lower values of the spectral index γ, the event rate is dominated by the highest neutrino energies. Consequently, the required values of $\mathcal{N}V$ are not highly sensitive to the energy threshold. For higher values of the spectral index, the steep dependence of flux on neutrino energy means that the event rate will be dominated by the lowest detected energies, near the threshold. This is evidenced by the more than ten orders of magnitude range in $\mathcal{N}V$ for the range of thresholds considered.

For a given effective detector volume V and energy threshold E_ν^{min}, the value of $\mathcal{N}_{\mathrm{min}}$ as a function of γ can be obtained from the graph in Fig. 5. An acoustic detector like DUMAND with $V = 100\ \mathrm{km}^3$ and $E_\nu^{\mathrm{min}} = 10^{17}$ eV is sensitive to $\mathcal{N} > 10^{35}$ when $\gamma = 4$, and $\mathcal{N} > 3 \cdot 10^{14}$ when $\gamma = 1.5$.

Alternatively, given a definite neutrino spectrum, one may determine the detector characteristics necessary to bring it under investigation. Consider as an example the model of Hill, Schramm, and Walker[8] for the isotropic neutrino flux arising from the disintegrations of superconducting cosmic strings into heavy fermions which themselves subsequently decay. The neutrino flux is influenced both by the mass of the heavy fermion and by the history of the magnetic field of the Universe. The magnetic field strength is taken to be related to redshift z as

$$B(z) = B_0 \cdot (1+z)^{-p+\frac{3}{2}}, \tag{5.2}$$

where the present value of the cosmic magnetic field is $B_0 = 10^{-9}$ gauss. For a fermion mass $m_F = 10^{15}\ \mathrm{GeV}/c^2$ suggested by theories of electronuclear unification and $p = -\frac{1}{2}$, the flux of electron-neutrinos and antineutrinos is characterized by $\mathcal{N} \simeq 5 \cdot 10^{16}$ and $\gamma = 1.5$ up to energies greater than 10^{21} eV. The flux of muon-neutrinos is about the same.[24] A detector with energy threshold $E_\nu^{\mathrm{min}} = 10^{17}$ eV requires a volume of $\sim 1\ \mathrm{km}^3$ to see one upward ν_e event per year, and only about $10^{-1}\ \mathrm{km}^3$ to see one downward ν_e event per year. The Fly's Eye detector already constrains the neutrino flux, as remarked in Ref. 8.

The Fly's Eye observations place an upper limit on the quantity

$$\mathcal{I}(E_\nu^{\min}) \equiv \int_{E_\nu^{\min}} dE_\nu \, \sigma_{\nu N}(E_\nu)\, j_\nu(E_\nu). \tag{5.3}$$

For downward going events, $\mathcal{I}(E_\nu^{\min} = 10^{17}\ \text{eV}) < 10^{-45}(\text{sec sr})^{-1}$, $\mathcal{I}(E_\nu^{\min} = 10^{18}\ \text{eV}) < 3.8 \cdot 10^{-46}(\text{sec sr})^{-1}$, and $\mathcal{I}(E_\nu^{\min} = 10^{19}\ \text{eV}) < 10^{-46}(\text{sec sr})^{-1}$.[25] By scaling out the cross section at the detection threshold, we define the convenient quantity

$$\overline{\Phi}(E_\nu^{\min}) \equiv \frac{1}{\sigma_{\nu N}(E_\nu^{\min})} \int_{\text{downward}} d\Omega \int_{E_\nu^{\min}} dE_\nu \, \sigma_{\nu N}(E_\nu)\, j_\nu(E_\nu). \tag{5.4}$$

In Fig. 6 we plot versus $E_\nu^{\min}$ the Fly's Eye upper bound on $\overline{\Phi}$, computed using our evaluation of the neutrino-nucleon cross section. We also plot $\overline{\Phi}$ for several models of neutrino fluxes: neutrinos from the point source Cygnus X-3,[3] atmospheric neutrinos,[23] and neutrinos arising from the decay of superconducting cosmic strings,[8] for $p = -\frac{1}{2}$ and 0.

At energies accessible to the Fly's Eye, atmospheric neutrinos are not a significant background to those arising from the disintegration of superconducting cosmic strings. The spectrum calculated under the assumption that $p = -\frac{1}{2}$, which corresponds to a cosmic magnetic field that scales with radiation (energy) density, is excluded[8] by the combination of the Fly's Eye upper limits and our evaluation of the neutrino cross section. The dashed line in Fig. 6 shows the level at which a 1 km^3 water detector would yield one event per year. On average over the energy range covered, the effective volume of the Fly's Eye is about 0.2 km^3 water equivalent. To push the sensitivity of such an apparatus down to the $p = 0$ event rate would require a volume of about 10 km^3 for downward neutrinos, and about 100 km^3 for the detection of upward neutrinos.

We also show in Fig. 6 the cross-section weighted flux for bright-phase models with $\bar{z} = 4$ and 6, with $\gamma_i = 1.5$ and 2.5. A 1 km^3 detector volume could detect the neutrino flux associated with the most optimistic bright phase model with $\bar{z} = 6$ and $\gamma_i = 1.5$, as we have demonstrated in Sec. IV. The dashed lines in Fig. 6 indicating other choices of $(\bar{z}, \gamma_i)$ exhibit graphically some of the results of Tables 2 and 3. Volumes on the order of 3–100 km^3 are required to detect such fluxes.

For completeness, we have included in Fig. 6 the cross-section-weighted flux $\overline{\Phi}$ for a point source. Assuming[26] that collisions of protons accelerated by Cygnus X-3 with the envelope of the companion star produce pions which ultimately yield a photon spectrum with index $\gamma = 2$, Gaisser and Stanev[3] have made a theoretical calculation of the period averaged differential flux of muon neutrinos at the surface of the earth. This neutrino flux enters into the expression for $\overline{\Phi}$. It is straightforward to make a comparison of point sources and isotropic sources in terms of $\overline{\Phi}$. Below $E_\nu^{min} \simeq 10^{14}$ eV, a detector volume much less than 1 km^3 is adequate for detecting neutrinos from Cygnus X-3, however, atmospheric neutrinos present a serious background problem.

VI. CONCLUSIONS

We have calculated cross sections for charged current and neutral current interactions of UHE neutrinos. By combining these cross sections with models for cosmic neutrino sources, we have made a quantitative evaluation of the water equivalent effective volume required to detect UHE neutrinos of both conventional and exotic origin. Detection with effective volumes on the order of $10 - 100$ km^3 can place significant constraints on bright phase models of galactic evolution and on the superconducting cosmic string scenario for galaxy formation.

We thank C. T. Hill, P. Sokolsky, T. Gaisser, T. Stanev and F. Halzen for advice and comments. We acknowledge the contributions of T. Walker to the first stages of this work.

FOOTNOTES AND REFERENCES

[1] K. Hirata, *et al.*, *Phys. Rev. Lett.* **58**, 1490 (1987); R. M. Bionta, *et al.*, *ibid.* **58**, 1494 (1987); see also W. Aglietta, *et al.*, "Characteristics of a Neutrino Burst Detected During the Occurrence of Supernova 1987a."

[2] E. W. Kolb, M. S. Turner, and T. P. Walker, *Phys. Rev. D***32**, 1145 (1985).

[3] T. K. Gaisser and T. Stanev, *Phys. Rev. Lett.* **54**, 2265 (1985).

[4] A. Dar, *Phys. Lett.* **159B**, 102 (1985); S. Berezinsky, C. Castagnoli, and

P. Galeotti, *Nuovo Cim.* **8C**, 187 (1985).

[5] M. Samorski and W. Stamm, *Astrophys. J. Lett.* **268**, L17 (1983); J. Lloyd-Evans, *et al.*, *Nature (London)* **305**, 784 (1983); R. J. Protheroe, R. W. Clay, and P. R. Gerhardy, *Astrophys. J. Lett.* **280**, L47 (1984).

[6] V. Berezinsky and G. Zatsepin, *Proceedings of the 1976 DUMAND Summer Workshop,* edited by A. Roberts and R. Donaldson (Fermilab, Batavia, Illinois, 1977) p. 215.

[7] C. T. Hill and D. N. Schramm, *Phys. Lett.* **131B**, 247 (1983); *Phys. Rev. D***31**, 564 (1985).

[8] C. T. Hill, D. N. Schramm, and T. P. Walker, Fermilab-Pub-86/146-T, *Phys. Rev. D***35**, xxx (1987). The superconducting cosmic string scenario for galaxy formation was elaborated by J. P. Ostriker, C. Thompson and E. Witten, *Phys. Lett.* **180B**, 231 (1986).

[9] D. W. McKay and J. P. Ralston, *Phys. Lett.* **167B**, 103 (1986).

[10] C. Quigg, M. H. Reno, and T. P. Walker, *Phys. Rev. Lett.* **57**, 774 (1986).

[11] Yu. M. Andreev, V. S. Berezinsky, and A. Yu. Smirnov, *Phys. Lett.* **84B**, 247 (1979).

[12] T. K. Gaisser and A. F. Grillo, "Evolution of structure functions and upward neutrino-induced muon signal in underground experiments," Frascati

preprint, July 1986 (unpublished).

[13] E. Eichten, I. Hinchliffe, K. Lane, and C. Quigg, *Rev. Mod. Phys.* **56**, 579 (1984). We use the revised distributions reported in *Rev. Mod. Phys.* **58**, 1065 (1986), which correct numerical errors in the heavy-quark evolution. See also J. C. Collins and Wu-Ki Tung, *Nucl. Phys.* **B278**, 934 (1986).

[14] The convenient analytic parametrizations of D. Duke and J. F. Owens, *Phys. Rev. D*30, 49 (1984) are not ideal for present purposes because they assume an $SU(3)$-symmetric sea.

[15] L. V. Gribov, E. M. Levin, and M. G. Ryskin, *Phys. Rep.* **100**, 1 (1983).

[16] G. P. Lepage, *J. Comput. Phys.* **27**, 192 (1978); Cornell report CLNS-80/447 (unpublished).

[17] L. S. Durkin and P. Langacker, in Particle Data Group, *Phys. Lett.* **170**, 1 (1986).

[18] We thank R. Silberberg for bringing this possibility to our attention.

[19] See *Proceedings of the La Jolla Workshop on Acoustic Detection of Neutrinos,* edited by H. Bradner, University of California, San Diego, 1977, and other volumes of the DUMAND summer workshop proceedings.

[20] The original observation is due to K. Greisen, *Phys. Rev. Lett.* **16**, 748

(1966), and to G. T. Zatsepin and V. A. Kuz'min, *Pis'ma Zh. Eksp. Teor. Fiz.* **4**, 114 (1966) [English transl.: *JETP Lett.* **4**, 78 (1966)].

[21] A. M. Hillas, *Can. J. Phys.* **46**, 5626 (1968); V. Berezhinsky and G. T. Zatsepin, *Yad. Fiz.* **11**, 200 (1970) [*Sov. J. Nucl. Phys.* **11**, 111 (1970)]; P. J. E. Peebles, *Astrophys. J.* **147**, 868 (1967).

[22] J. Linsley, in *Proceedings of the Thirteenth International Conference on Cosmic Rays, Denver, 1973* (Colorado Associated University Press, Boulder, 1973), Vol. 5, p. 3207, and *Proceedings of the Fourteenth International Conference on Cosmic Rays, Munich, 1975,* edited by Klaus Pinkau (Max-Planck-Institut, Munich, 1975), p. 598, and *Proceedings of the 18th International Cosmic Ray Conference , Bangalore, India,* edited by N. Durgaprasad, *et al.*(Tata Institute of Fundamental Research, Bombay, 1983); G. Cunningham, *et al.*, *Astrophys. J. Lett.* **236**, L71 (1980); R. M. Baltrusaitis, *et al.*, *Phys. Rev. Lett.* **54**, 1875 (1985).

[23] L. V. Volkova, *Yad. Fiz.* **31**, 1510 (1980) [*Sov. J. Nucl. Phys.* **31**, 784 (1980)].

[24] C. T. Hill, private communication.

[25] R. M. Baltrusaitis, *et al.*, *Phys. Rev. D***31**, 2192 (1985).

[26] A. M. Hillas, *Nature (London)* **312**, 50 (1984).

Table 1: Events per year initiated by a diffuse cosmic neutrino flux produced by interactions of the observed cosmic-ray proton spectrum (at redshift $\bar{z} = 0$) for a volume of water 100 km^3 at a depth of 4000 m.w.e. The acoustic detector is assumed sensitive to the interactions of neutrinos with $E_\nu > 10^{17}$ eV. The results for $E_\nu > 10^{16}$ eV are larger by no more than 1%.

γ_i	Without shadowing	With shadowing
1.5	$2.0 \cdot 10^{-1}$	$1.0 \cdot 10^{-1}$
1.8	$8.7 \cdot 10^{-2}$	$4.4 \cdot 10^{-2}$
2.0	$5.3 \cdot 10^{-2}$	$2.7 \cdot 10^{-2}$
2.2	$2.9 \cdot 10^{-2}$	$1.5 \cdot 10^{-2}$
2.5	$1.2 \cdot 10^{-2}$	$6.0 \cdot 10^{-3}$
3.0	$1.2 \cdot 10^{-3}$	$6.1 \cdot 10^{-4}$

Table 2: Events per year initiated by a diffuse cosmic neutrino flux in a bright phase model with $\bar{z} = 4$ for a volume of water 100 km^3 at a depth of 4000 m.w.e. The acoustic detector is assumed sensitive to the interactions of neutrinos with $E_\nu > 10^{17}(10^{16})$ eV.

γ_i	Without shadowing	With shadowing
1.5	$1.5 \cdot 10^{+2}$ ($1.7 \cdot 10^{+2}$)	$7.9 \cdot 10^{+1}$ ($8.8 \cdot 10^{+1}$)
1.8	$6.5 \cdot 10^{+1}$ ($7.2 \cdot 10^{+1}$)	$3.4 \cdot 10^{+1}$ ($3.8 \cdot 10^{+1}$)
2.0	$4.0 \cdot 10^{+1}$ ($4.4 \cdot 10^{+1}$)	$2.1 \cdot 10^{+1}$ ($2.3 \cdot 10^{+1}$)
2.2	$2.2 \cdot 10^{+1}$ ($2.4 \cdot 10^{+1}$)	$1.2 \cdot 10^{+1}$ ($1.3 \cdot 10^{+1}$)
2.5	8.8 (9.8)	4.7 (5.2)
3.0	$9.0 \cdot 10^{-1}$ (1.0)	$4.8 \cdot 10^{-1}$ ($5.3 \cdot 10^{-1}$)

Table 3: Events per year initiated by a diffuse cosmic neutrino flux in a bright phase model with $\bar{z} = 6$ for a volume of water 100 km^3 at a depth of 4000 m.w.e. The acoustic detector is assumed sensitive to the interactions of neutrinos with $E_\nu > 10^{17}(10^{16})$ eV.

γ_i	Without shadowing	With shadowing
1.5	$1.1\cdot10^{+3}$ $(1.3\cdot10^{+3})$	$5.8\cdot10^{+2}$ $(7.3\cdot10^{+2})$
1.8	$4.7\cdot10^{+2}$ $(5.8\cdot10^{+2})$	$2.5\cdot10^{+2}$ $(3.2\cdot10^{+2})$
2.0	$2.9\cdot10^{+2}$ $(3.6\cdot10^{+2})$	$1.5\cdot10^{+2}$ $(1.9\cdot10^{+2})$
2.2	$1.6\cdot10^{+2}$ $(2.0\cdot10^{+2})$	$8.4\cdot10^{+1}$ $(1.1\cdot10^{+2})$
2.5	$6.4\cdot10^{+1}$ $(8.0\cdot10^{+1})$	$3.5\cdot10^{+1}$ $(4.4\cdot10^{+1})$
3.0	6.8 (8.4)	3.6 (4.6)

FIGURE CAPTIONS

Figure 1: (a) Cross sections for νN interactions at high energies. Dotted line: $\sigma(\nu N \rightarrow \mu X)$, dashed line: $\sigma(\nu N \rightarrow \nu X)$, solid line: total (charged current plus neutral current) cross section. (b) Same quantities for $\bar{\nu} N$ interactions.

Figure 2: Interaction lengths in earth for neutrinos. Dotted line: charged current interaction length, dashed line: neutral current interaction length, solid line: total interaction length. The heavy horizontal line indicates one earth diameter.

Figure 3: Shadowing factor (3.2) for a detector on the earth's surface, integrated over azimuth, as a function of the zenith angle θ, for neutrinos of 10^{13}, 10^{15}, 10^{17}, and 10^{19} eV incident on the earth. Half the upward flux lies between 90° and the angles indicated by black dots.

Figure 4: Spectrum $j_{\nu}(E_{\nu})$ of cosmic electron-neutrinos for injection spectra with indices $\gamma_i = 1.5, 2.0$, and 2.5 produced at characteristic redshifts $\bar{z} = 0, 4$, and 6. [After Hill and Schramm, Ref. 7.] The spectrum of muon-neutrinos is approximately the same.

Figure 5: Dependence on neutrino spectral index of the effective detector volume V times flux normalization $\mathcal{N}$ required for one interaction of an upward

going (solid lines) or downward going (dashed lines) neutrino per year for detector thresholds represented as cuts on minimum neutrino energy between 10^{10} and 10^{19} eV.

Figure 6: The cross-section-weighted flux $\overline{\Phi}(E_\nu^{\min})$ as a function of the minimum neutrino energy required for detection, for various sources of high energy neutrinos. Dashed lines are for bright-phase models labeled by $(\bar{z}, \gamma_i)$. The atmospheric ν_μ or $\overline{\nu}_\mu$ flux is from Ref. [23]. The fluxes for disintegrating superconducting cosmic strings (SCCS) refer to electron-neutrinos or antineutrinos. The corresponding muon-neutrino fluxes are approximately the same. The bold solid line is the upper limit[25] for $\nu_e \rightarrow e$ interactions from the Fly's Eye detector. The ν_μ or $\overline{\nu}_\mu$ flux for the point source Cyg X-3 is taken from Ref. [3]. The dotted line indicates the flux for which a 1 km^3 water detector would register one event per year above the specified neutrino energy threshold.

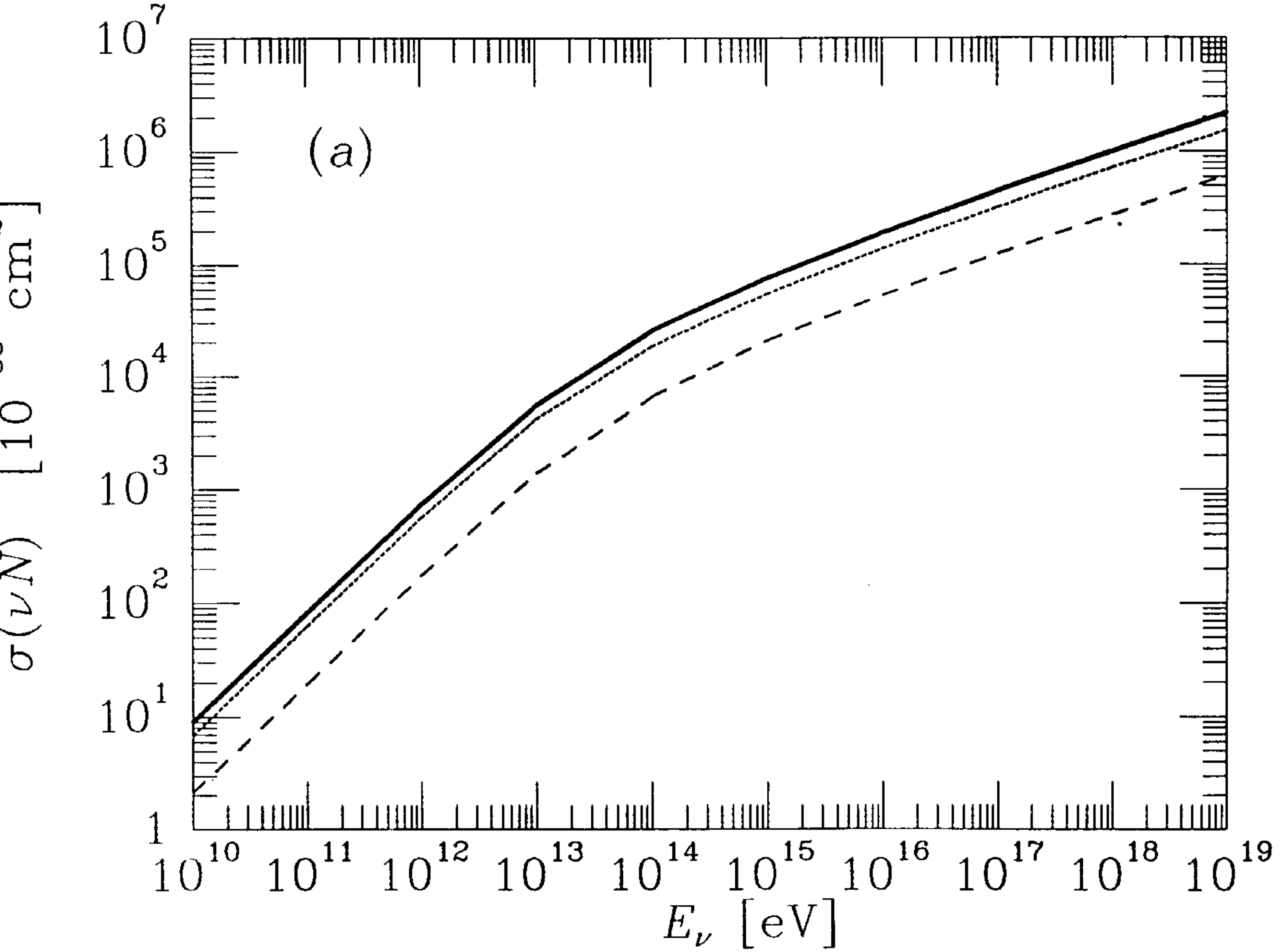
(a)
$\sigma(\nu N)$ $[10^{-38}$ cm$^2]$
10^7
10^6
10^5
10^4
10^3
10^2
10^1
1
10^{10}
10^{11}
10^{12}
10^{13}
10^{14}
10^{15}
10^{16}
10^{17}
10^{18}
10^{19}
E_ν [eV]

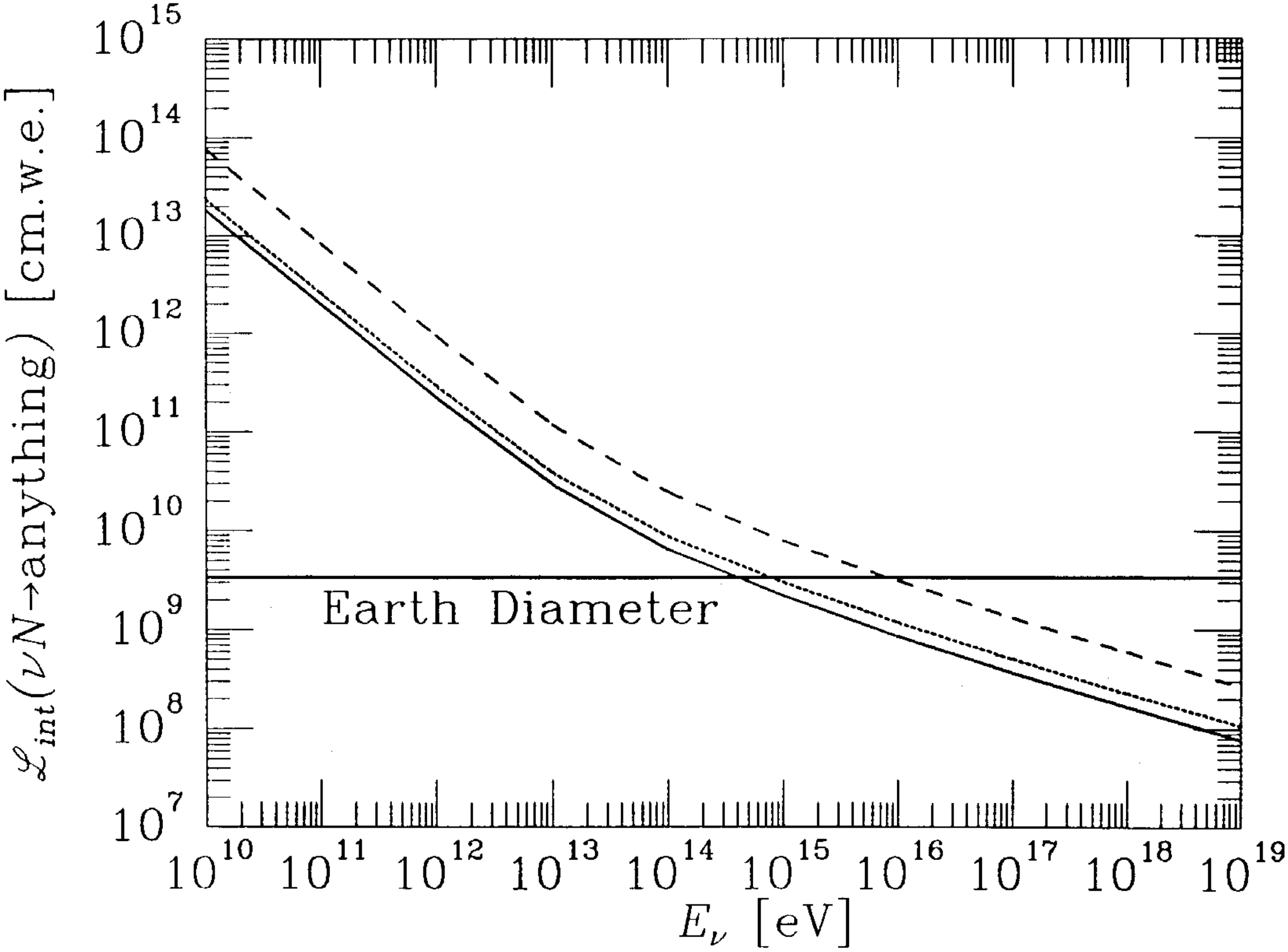
$\mathscr{L}_{int}(\nu N \to \text{anything})$ [cm.w.e.]
10^{7}
10^{8}
10^{9}
10^{10}
10^{11}
10^{12}
10^{13}
10^{14}
10^{15}
Earth Diameter
10^{10}
10^{11}
10^{12}
10^{13}
10^{14}
10^{15}
10^{16}
10^{17}
10^{18}
10^{19}
E_ν [eV]

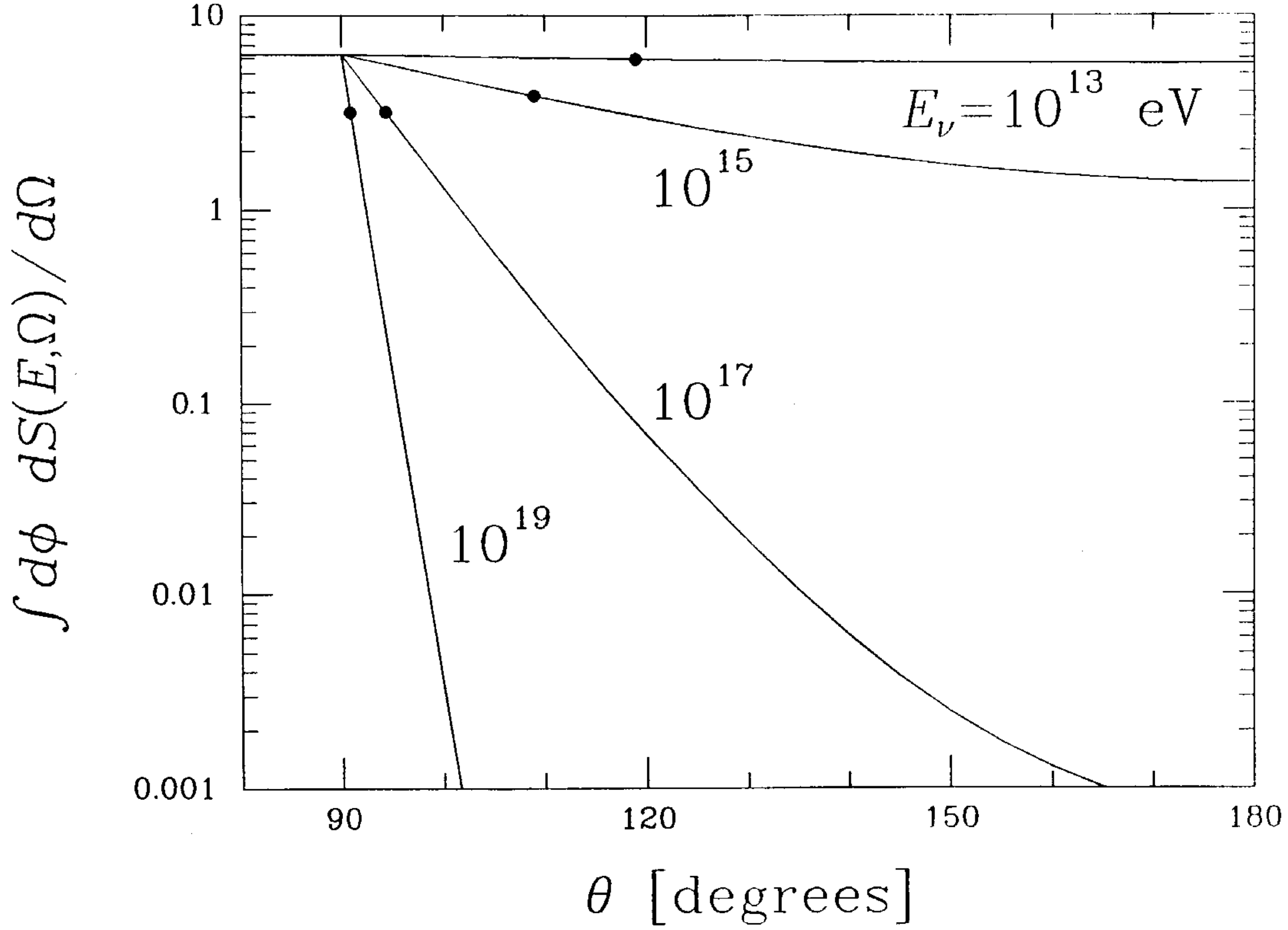
10
1
0.1
0.01
0.001
90
120
150
180
$\int d\phi \;\; dS(E,\Omega)/d\Omega$
θ [degrees]
$E_\nu = 10^{13}$ eV
10^{15}
10^{17}
10^{19}

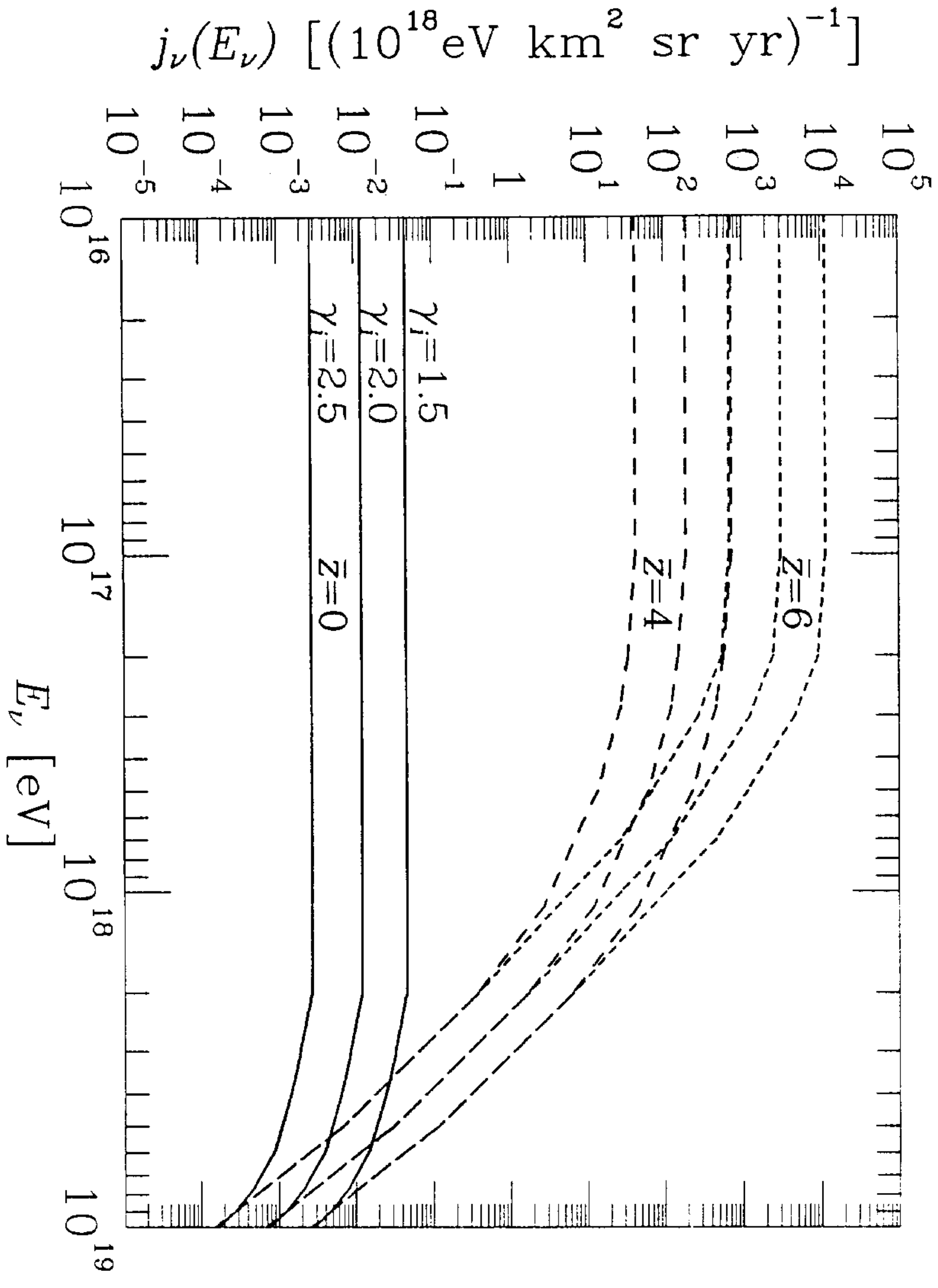

$j_\nu(E_\nu)$ $[(10^{18}\mathrm{eV\ km^2\ sr\ yr})^{-1}]$
10^{5}
10^{4}
10^{3}
10^{2}
10^{1}
1
10^{-1}
10^{-2}
10^{-3}
10^{-4}
10^{-5}
10^{16}
10^{17}
10^{18}
10^{19}
E_ν [eV]
$\gamma_i=1.5$
$\gamma_i=2.0$
$\gamma_i=2.5$
$\bar{z}=0$
$\bar{z}=4$
$\bar{z}=6$

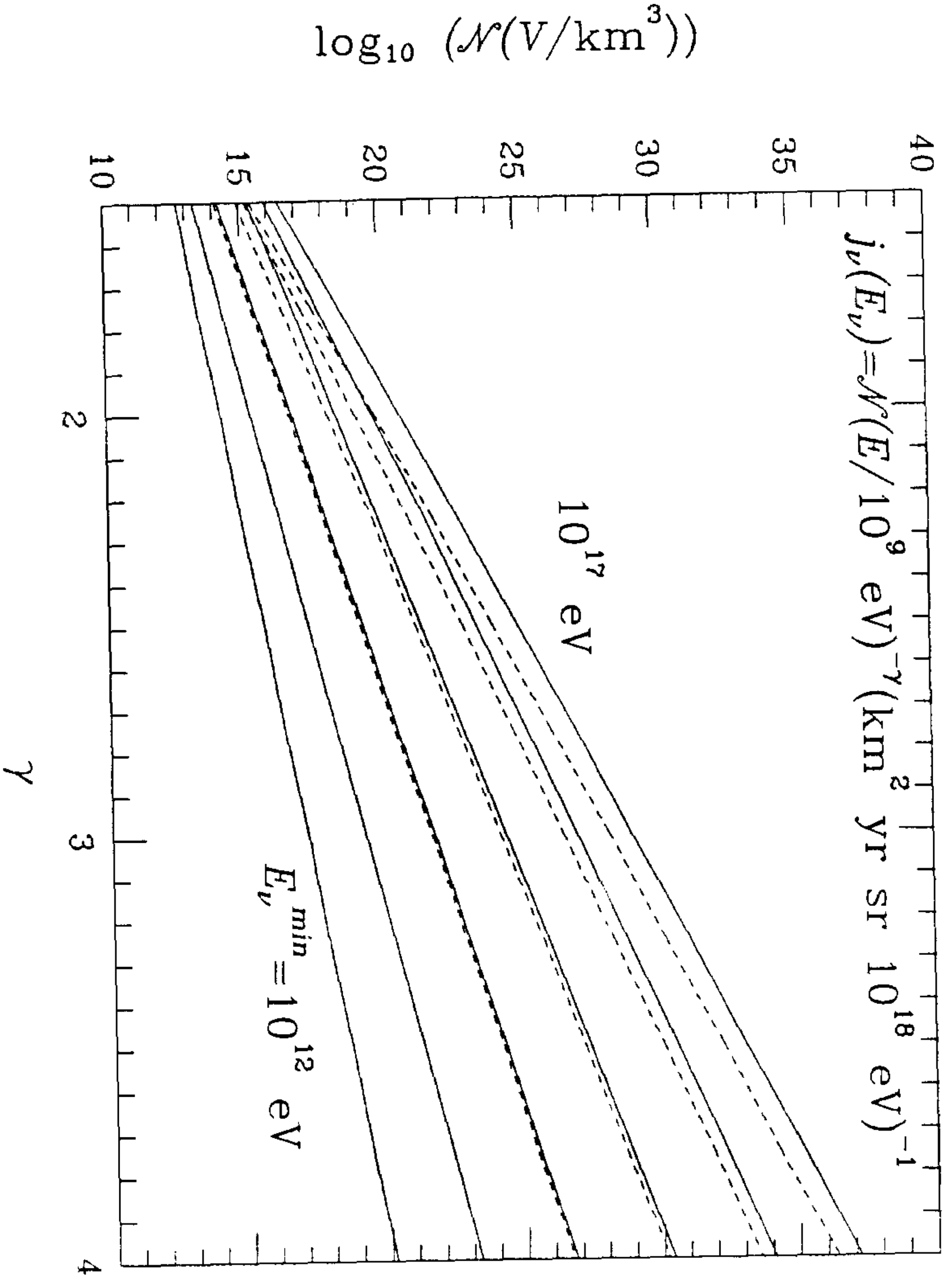

$\log_{10}\ (\mathcal{N}(V/\mathrm{km}^3))$
$j_\nu(E_\nu)=\mathcal{N}(E/10^9\ \mathrm{eV})^{-\gamma}(\mathrm{km}^2\ \mathrm{yr\ sr}\ 10^{18}\ \mathrm{eV})^{-1}$
10^{17} eV
$E_\nu^{min}=10^{12}$ eV
γ
10
15
20
25
30
35
40
2
3
4

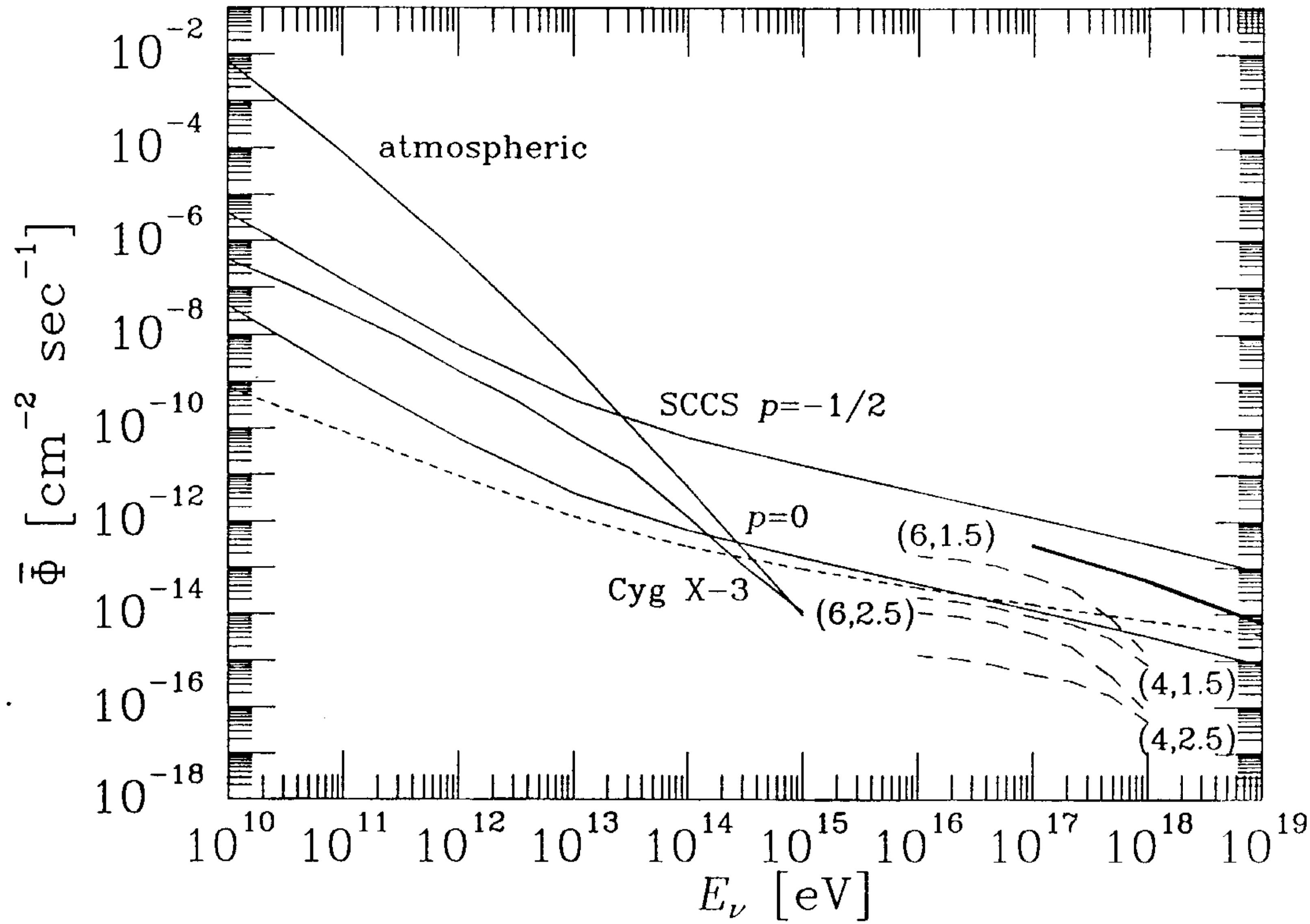
$\bar{\Phi}$ [cm^{-2} sec^{-1}]
10^{-2}
10^{-4}
10^{-6}
10^{-8}
10^{-10}
10^{-12}
10^{-14}
10^{-16}
10^{-18}
atmospheric
SCCS p=−1/2
p=0
Cyg X−3
(6,1.5)
(6,2.5)
(4,1.5)
(4,2.5)
10^{10}
10^{11}
10^{12}
10^{13}
10^{14}
10^{15}
10^{16}
10^{17}
10^{18}
10^{19}
E_ν [eV]